JMEPEG (2006) 15:699-704
DOI: 10.1361/105994906X150713

1059-9495/$19.00

# Comparative Characteristic and Erosion Behavior of NiCr Coatings Deposited by Various High-Velocity Oxyfuel Spray Processes

*Hazoor Singh Sidhu, Buta Singh Sidhu, and S. Prakash*

*(Submitted March 19, 2005; in revised form April 24, 2006)*

**The purpose of this study is to analyze and compare the mechanical properties and microstructure details at the interface of high-velocity oxyfuel (HVOF)-sprayed NiCr-coated boiler tube steels, namely ASTM-SA-210 grade A1, ASTM-SA213-T-11, and ASTM-SA213-T-22. Coatings were developed by two different techniques, and in these techniques liquefied petroleum gas was used as the fuel gas. First, the coatings were characterized by metallographic, scanning electron microscopy/energy-dispersive x-ray analysis, x-ray diffraction, surface roughness, and microhardness, and then were subjected to erosion testing. An attempt has been made to describe the transformations taking place during thermal spraying. It is concluded that the HVOF wire spraying process offers a technically viable and cost-effective alternative to HVOF powder spraying process for applications in an energy generation power plant with a point view of life enhancement and to minimize the tube failures because it gives a coating having better resistance to erosion.**

**Keywords** high-velocity oxyfuel, microstructure, NiCr powder, NiCr wire

## 1. Introduction

Alloys that are used at high temperature should possess good mechanical properties along with erosion-corrosion resistance. However, it is impossible for a single material to have all these properties, along with ease of manufacturing. Therefore, a composite system using a base material providing the necessary mechanical strength with a protective surface layer that is different in structure and/or chemical composition can be an optimum choice in combining material properties (Ref 1).

There is increased attention on the energy conversion efficiency of power plants to meet the need of industries along with ensuring plant reliability, availability, and maintainability. Coating technology is progressing at a steady rate with continuous improvements in coating performance. But performance alone is not sufficient to determine the success of a new technology, and it must be balanced against cost and environmental impact. So, the use of different methods for depositing the same coatings may lead to very different results in terms of the quality/cost ratio (Ref 2).

The high-velocity oxyfuel (HVOF) process is reported to be a versatile technology and has been adopted by many industries due to its flexibility, cost-effectiveness, and the superior quality of coating produced. This spraying process has been designed to retain the characteristics of the coating. The hypersonic velocity of the flame shortens the time of interaction between the powder and flame, whereas the low temperature of the substrate limits the grain growth and decomposition of the coating. Due to the high impact velocity of particles, the coatings show a high adhesive strength, high cohesive strength of individual splats, uniform microstructure, high density, and low porosity (Ref 3-6). The various HVOF systems differ in their design based on the use of water or air cooling, axial or radial powder injection, wire or powder spraying, fuel flows and composition, combustion chamber pressure and configuration, powder injection location, and nozzle design and length. The combustion fuels include propylene, propane, natural gas, hydrogen, acetylene, liquefied petroleum gas (LPG), and kerosene. This wide range of fuels permits the selection of the most economical fuel to produce the required coating characteristics.

The thermal sprayed 50/50 nickel-chromium alloy is usually recommended as an erosion-corrosion protection for boiler tubes in power generation applications (Ref 7). As reported by Sundararajan et al. (Ref 8, 9), the pure metal oxides of Ni- and Co-base alloys are not protective enough when the working temperature exceeds 550 °C. The addition of other elements, namely Cr, Al, and Si, have improved their corrosion resistance due to the establishment of more protective oxide layers such as $Cr_2O_3$, $Al_2O_3$, or $SiO_2$, respectively. They further reported that the thick and dense HVOF-deposited NiCr coatings yield a better steam oxidation resistance than the thin porous air plasma spray-deposited NiCr coatings.

Hearley et al. (Ref 10) evaluated the erosion behavior of the NiAl intermetallic coatings produced by the HVOF spray process. They concluded that the mass loss varies with velocity and the angle of impingement. The microstructure and solid particle erosion resistance of FeCrAlY-$Cr_3C_2$ and NiCr-$Cr_3C_2$ cermet coatings with carbide levels ranging from 1 to 100% (in the prespray powder) have been evaluated by Stein et al. (Ref

**Hazoor Singh Sidhu,** Department of Mechanical Engineering, Yadvindra College of Engineering, Punjabi University, Guru Kashi Campus, Talwandi Sabo, Bathinda, Punjab-151302, India; **Buta Singh Sidhu,** Department of Mechanical Engineering, Giani Zail Singh College of Engineering and Technology, Bathinda, Punjab-151001, India; and **S. Prakash,** Department of Metallurgical and Materials Engineering, Indian Institute of Technology, Roorkee-247667, India. Contact e-mail: hazoors@yahoo.com.

**Table 1 Chemical composition (wt.%) for various boiler tube steels**

| Type of steel | C | Mn | Si | S | P | Cr | Mo | Fe |
|---|---|---|---|---|---|---|---|---|
| GrAl | 0.27 | 0.93 | 0.1 | 0.058 | 0.048 | … | … | Balance |
| T-11 | 0.15 | 0.3–0.6 | 0.5–1 | 0.03 | 0.03 | 1–15 | 0.44–0.65 | Balance |
| T-22 | 0.15 | 0.3–0.6 | 0.5 | 0.03 | 0.03 | 1.9–2.6 | 0.87–1.13 | Balance |

11) with a point of view of determining the optimum ceramic content for the best erosion resistance.

## 2. Experimental Method

### 2.1 High-Velocity Oxyfuel Deposition

Three types of boiler tube steels, low carbon steel ASTM-SA210 grade A1 (GrA1), 1Cr-0.5Mo steel ASTM-SA213-T-11 (T110), and 2.25Cr-1Mo steel ASTM-SA213-T-22 (T22), were used as substrate steels. The chemical composition of these steels is shown in Table 1. These steel samples were cut to form specimens approximately $3 \times 15 \times 15$ mm$^3$ in size. The specimens were polished and grit-blasted with $Al_2O_3$ (grit 45) before coating.

Coatings were developed at M/S MEC (Jodhpur, India) by using two types of commercial equipment. The Hipojet-2100 was used for powder spraying and the Hijet-9600 was used for wire spraying; this equipment was operated using oxygen and LPG gases. The chemical compositions of the coating materials were 80 wt.% Ni and 20 wt.% Cr. The spraying parameters are given in Table 2. The substrate steels were cooled with compressed air jets during and after spraying. After coating, the specimens were sectioned, mounted, and polished for metallurgical examination along the cross section. Scanning electron microscopy (SEM) analysis, energy-dispersive x-ray analysis (EDAX), and x-ray diffraction (XRD) techniques were then used to analyze various constituents of the coatings. The cross-sectional microhardness was evaluated using a microhardness tester (HMV-2 series; Mitsubishi, Tokyo, Japan). Surface roughness and porosity were also evaluated for all of the coated steels.

### 2.2 Erosion Testing

The solid particle erosion tests were performed on an air jet erosion tester (IIT, Delhi, India) by using 150 to 200 μm angular silica sand particles, according to the ASTM G76 (Ref 12) standard. A particle feed rate of 50 g/min was used for a total of 8 kg of sand to achieve the steady-state conditions. The particles were propelled at 28 m/s from a barrel 3 mm in diameter onto the target coatings 10 mm from the nozzle. Impingement angles of 30° and 90° were selected to provide the severe erosion conditions for both ductile and brittle materials (Ref 11). Weight loss was measured, and the results are reported as the weight of the material eroded per unit weight of the erodent particles (called the specific erosion rate in grams per gram) used during the test.

## 3. Experiment Results

### 3.1 Coating Thickness, Porosity, and Surface Roughness Measurement

The thicknesses of the coatings have been measured with a traveling microscope at 100× magnification. The coating thicknesses reported in Table 3 were close to the desired coating thickness.

**Table 2 Spray parameters employed during HVOF spraying**

| Parameters | Hijet-9600 (wire) | Hipojet-2100 (powder) |
|---|---|---|
| Oxygen flow rate, L/min | 250 | 250 |
| LPG flow rate, L/min | 60 | 70 |
| Air flow rate, L/min | 900 | 6200 |
| Spray distance, mm | 200 | 200 |
| Wire/powder feed rate, g/min | 80 | 30 |
| Wire diameter/particle size | 3.17 mm | −45 + 15 μm |

The porosity measurements for HVOF-sprayed coatings have been made with an image analyzer (Soft-Imaging System, Munster, Germany) at Research and Development Center TIET (Patiala, India). The porosity for as-sprayed NiCr wire and NiCr powder coatings was in the range of <1 and 2 to 3.5%, respectively. The surface roughness of each coating has been evaluated with a Surf-corder (SE-1200; Kosaka Laboratory, Ltd., Tokyo, Japan).

### 3.2 Microhardness Analysis

The microhardness of the substrate steels has been measured to be in the range of 200 to 280 Vickers hardness (Hv). The microhardness values of the NiCr powder and NiCr wire coatings have been observed to be ~400 Hv. The profile for microhardness versus distance from the coating-substrate interface is presented in Fig. 1.

### 3.3 Morphology of the Coatings

The optical micrograph of the NiCr wire coatings (Fig. 2b) indicates a uniformly distributed fine grain structure, whereas that of the NiCr powder coating indicates a coarse grain structure (Fig. 2a). Unmelted particles and inclusion can also be seen in the microstructure of the NiCr powder coating.

The optical microstructure along the cross section of the HVOF coating is shown in Fig. 3. Some oxide inclusions and porosity can be seen in the microstructures. The NiCr wire coatings have a uniform, fine, and layered structure, whereas the NiCr powder coating has a coarse and uniform structure.

### 3.4 Scanning Electron Microscopy/Energy-Dispersive X-Ray Analysis, and X-Ray Diffraction Analysis

From the SEM analysis/EDAX of the coatings, it can be inferred that there is a nickel-rich matrix. Some oxide inclusion and a thin, dark contrast stringer, which is rich in oxygen relative to the metallic matrix, have also been observed. The

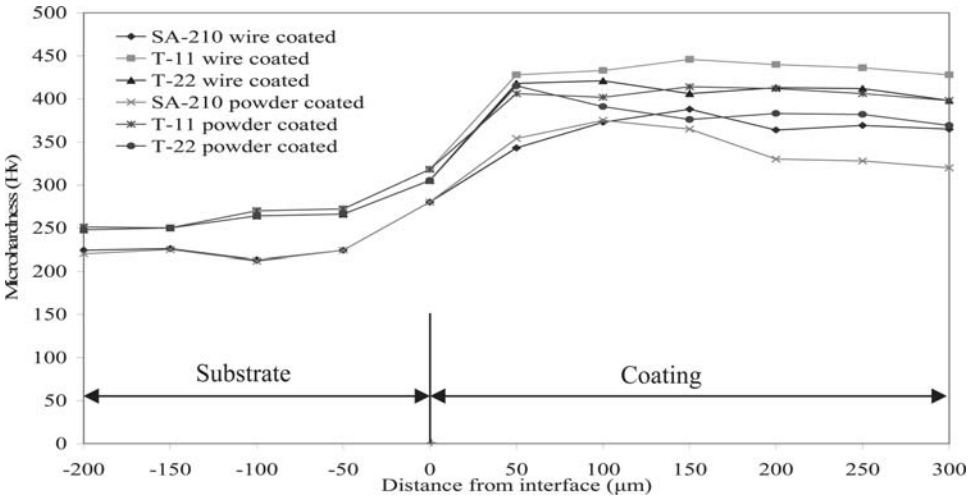


**Fig. 1** Microhardness profile for various steels after NiCr coating across the cross section

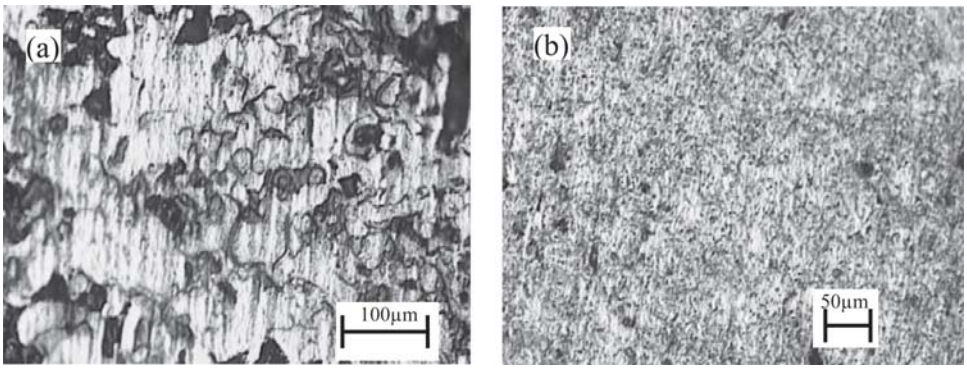


**Fig. 2** Optical micrograph of the surface of (a) NiCr powder-coated and (b) NiCr wire-coated steels

**Table 3 Coating characteristics**

| Type of coating | Coating thickness, μm | Roughness(a), μm | Porosity, % |
|---|---|---|---|
| NiCr (powder) | 300 | 6.889 ± 0.32 | 2–3.5 |
| NiCr (wire) | 330 | 5.536 ± 0.37 | <1 |

(a) Values are given as mean ± SD.

dark black spots are the pores in the coatings and substrate steels (Fig. 4). The XRD analysis for coatings, as indicated in Fig. 5, has major peaks of Ni, whereas small-intensity peaks of Cr have also been formed.

### *3.5 Erosive Wear*

The erosion rate of the coatings is presented in Fig. 6. The NiCr powder coating has a high erosion rate compared with the NiCr wire coating. However, a relatively higher erosion rate was observed at a 30° angle of impingement, which indicates that the coating erodes in a ductile manner. Figure 7(a) shows the larger damaged area, which is consistent with splat pullout, whereas the more wear-resistant NiCr wire coating (Fig. 7b) exhibited an evenly damaged area with no splat pullout.

## 4. Discussion

NiCr wire coatings have no unmelted or semimelted particles, because in the case of NiCr wire spraying only molten particles can detach from the wire, whereas in NiCr powder coatings the particles may not be fully melted. The microstructures show the presence of some oxide inclusions in the coatings (dark contrast phase) and reveal that most of this oxide is located at the interparticle boundaries. A thin, dark-contrast stringer corresponds to an oxide phase, with the higher amount of oxygen detected by EDAX. This oxide stringer is believed to be the result of the oxidation occurring at the surface of particles in flight as well as at the coating surface by the entrainment of atmospheric oxygen into the jet prior to the deposition of the next layer. A similar type of oxide phase at the interface boundary has also been observed by Dent et al. (Ref 13) and Sturgeon (Ref 14). The microstructures in the current study have many similarities to those in HVOF-sprayed NiCr coatings that have been reported elsewhere (Ref 8, 9, 13, 15). It is clear from Fig. 2 and 3 that the NiCr wire coating has a fine, layered, and uniform microstructure compared with some other coatings reported by Ak et al. (Ref 15), Hearley et al. (Ref 10) and Stein et al. (Ref 11).

In the case of the NiCr wire coating, a high proportion of the feedstock wire appeared to have fully melted prior to the impact on the substrate. The better microstructure integrity of the

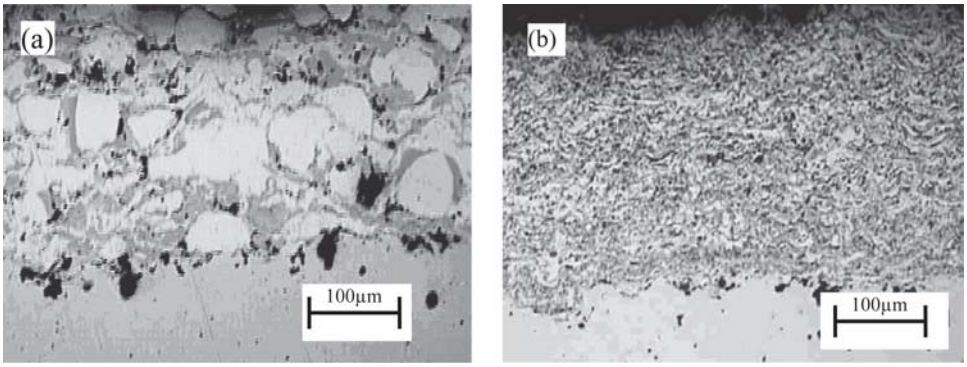


**Fig. 3** Optical micrograph along the cross section of (a) NiCr powder-coated steel and (b) NiCr wire-coated steel

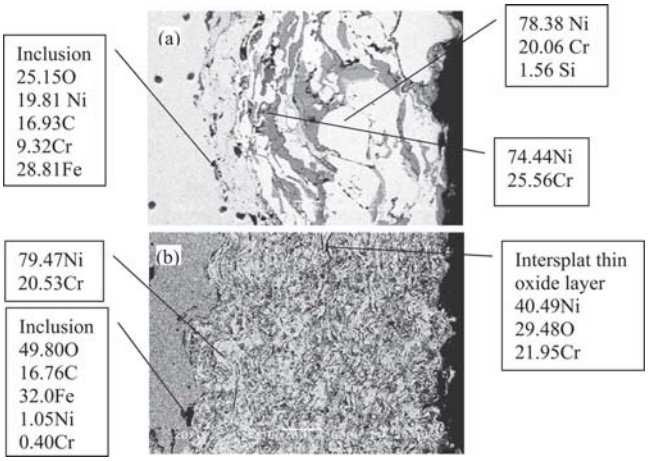


**Fig. 4** Back scattered electron imagery/EDAX analysis of a coating showing the elemental composition (wt.%) at various points along the cross section of (a) the NiCr powder coating and (b) the NiCr wire coating

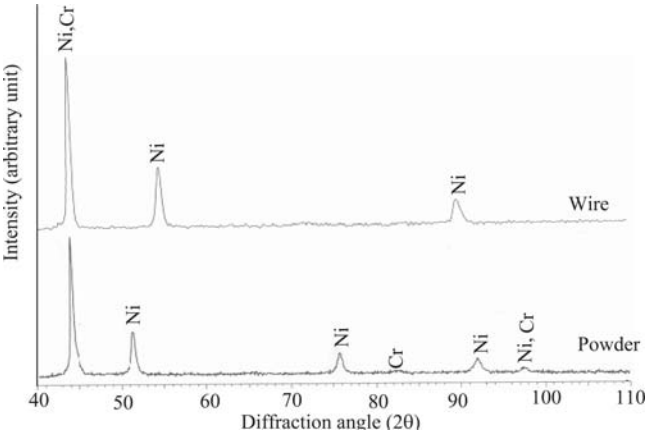


**Fig. 5** XRD spectra for NiCr-coated steel

NiCr wire coating may be due to the fact that material detached from the NiCr wire only after melting and the degree of plastic deformation was also large on impingement to the substrate. As a result, flattened and fine particles were formed. But in the case of powder, some unmelted or semimelted particles of the powder may be sprayed. These unmelted or semimelted powder particles decrease the splat-to-splat bonding and also increase the porosity, which might have contributed to the higher erosion rate of the coating. The coating has a dense, layered structure; the limited porosity is visible as very dark contrast regions. The porosity of the NiCr wire coating (<1%) is less than the porosity values reported by Sturgeon (Ref 14) and Ak et al. (Ref 15) for NiCr coatings.

The microhardness values of the coatings are measured to be greater than those of the substrate steels. A high microhardness value is believed to be due to the high kinetic energy acquired by the powder particles, which ensures good cohesion, and a denser and more homogeneous structure, as suggested by Verdon et al. (Ref 16) and Hawthorne et al. (Ref 17). The NiCr wire coating has uniform microhardness values of approximately 400 Hv, which is higher than the microhardness values reported by Ak et al. (Ref 15) for NiCr coatings. The microhardness values of the coatings are almost consistent with the findings of Uusitalo et al. (Ref 18).

X-ray diffractograms for the NiCr coating has confirmed the presence of higher amounts of Ni, the outstanding phase, because the powder has a composition of 80Ni and 20Cr. But, apart from the Ni, small-intensity peaks of Cr have also been observed. A peak of high intensity is indexed to both Ni and Cr, but a large number of peaks are indexed to Ni. Broad maxima in the range of 55 to 75 2θ seams to indicate an amorphous phase in the deposit. According to XRD analysis, very little transformation occurred during spraying, and NiCr did not undergo any decomposition during spraying. This result may be believed to be due to the higher flame velocity and lower flame temperature of the HVOF process, which would limit the decomposition process. The identical peaks observed in the current study have also been observed by Ak et al. (Ref 15) for NiCr coatings. The XRD results are further supported by SEM analysis/EDAX.

Microstructural characteristics of low porosity and oxides, fine splat size, good adhesion, and the absence of cracks are reported to enhance erosion resistance by Hearley et al. (Ref 10) and Wang and Lee (Ref 19). The porosity may initiate the microcracking, leading to the loss of lamella and thus to the removal of the coating. The low erosion rate of NiCr wire coating is closely correlated with their low porosity, and fine and uniform microstructure. The high erosion rate of the NiCr powder coating may be due to the coarse structure, because both of the coatings have approximately the same hardness values. These coatings showed a high erosion rate at a 30° angle of impingement, which corresponds to ductile erosion behavior. This may be due to the low shear strength of the coatings and their capability for absorbing the large amount of energy produced by the impinging particles at a 90° angle of

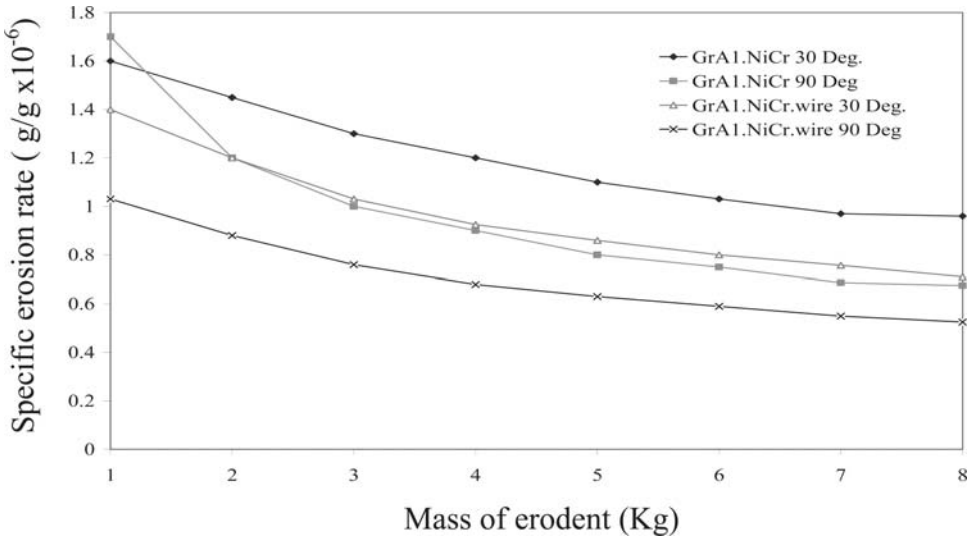


**Fig. 6** Specific erosion rate of NiCr coatings at 30° and 90° angle of impingement

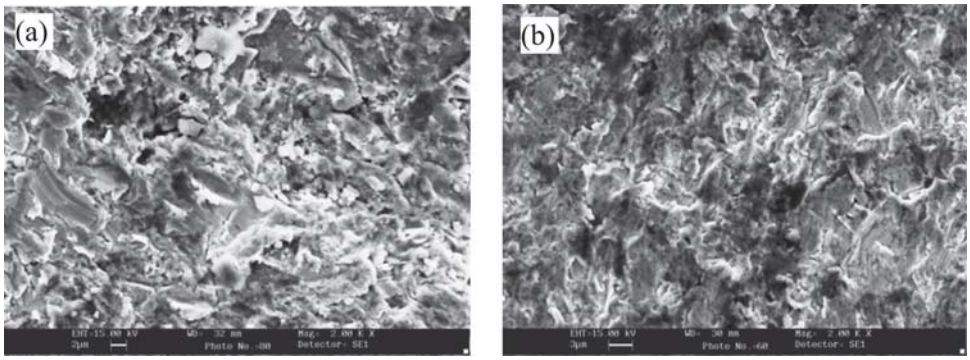


**Fig. 7** Typical appearance of the (a) NiCr powder coating and (b) NiCr wire coating after erosion at 30° impingement (2000×)

impingement (Ref 7). Hawthorne et al. (Ref 17) have also observed a higher wear rate at a low angle for ductile materials in dry erosion.

## 5. Conclusions

NiCr coatings were successfully obtained up to the thickness of ~300 to 330 μm by the HVOF process with LPG as fuel gas. The microhardness measurement across the cross section of the coating showed that the coatings have high hardness values compared with the substrate steels. Micrographs showed that NiCr powder coatings possess some semimelted particles, inclusions, oxides, and a coarse grain structure whereas the NiCr wire coatings possess a fine, layered, dense and uniform structure. The NiCr wire coating also has very low porosity compared with the NiCr powder coating. The NiCr wire coating has a higher erosion resistance compared with the NiCr powder coating.

### References


1. M.H. Li, Z.Y. Zhang, X.F. Sun, J.G. Li, F.S. Yin, W.Y. Hu, H.R. Guan, and Z.Q. Hu, Oxidation Behaviour of Sputter-Deposited NiCrAlY coating, *Surf. Coat. Technol.,* 2003, **165**(3), p 241-247
2. A. Scrivani, R. Groppetti, U. Bardi, A. Lavacchi, and G. Rizzi, A Comparative Study on HVOF, Vacuum Plasma Spray and Axial Plasma Spray for CoNiCrAlY Alloy Deposition, *Thermal Spray 2001: New Surfaces for a New Millennium,* C.C. Berndt, K.A. Khor, and E.F. Lugscheider, Ed., May 28-30, 2001 (Singapore), ASM International, 2001, p 561-565
3. A. Scrivani, S. Ianelli, A. Rossi, R. Groppetti, F. Casadei, and G. Rizzi, A Contribution to the Surface Analysis and Characterisation of HVOF Coatings for Petrochemical Application, *Wear,* 2001, **250,** p 107-113
4. D.A. Stewart, P.H. Shipway, and D.G. McCartney, Abrasive Wear Behaviour of Conventional and Nanocomposite HVOF-Sprayed WC–Co coatings, *Wear,* 1999, **225-229,** p 789-798
5. J.A. Picas, A. Forn, A. Igartua, and G. Mendoza, Mechanical and Tribological Properties of High Velocity Oxy-Fuel Thermal Sprayed Nanocrystalline CrC–NiCr Coatings, *Surf. Coat. Technol.,* 2003, **174-175,** p 1095-1100
6. S. Wirojanupatump, P.H. Shipway, and D.G. McCartney, The Influence of HVOF Powder Feedstock Characteristics on the Abrasive Wear Behaviour of CrxCy–NiCr Coatings, *Wear*, 2001, **249,** p 829-837
7. S. Gainger and J. Blunt, *Engineering Coatings: Design and Application,* Abington Publishing, Cambridge, U.K. 1998
8. T. Sundararajan, S. Kuroda, T. Itagaki, and F. Abe, Steam Oxidation Resistance of Ni-Cr Thermal Spray Coatings on 9Cr-1Mo Steel, Part-1, *ISIJ Int.,* 2003, **43,** p 95-103
9. T. Sundararajan, S. Kuroda, T. Itagaki, and F. Abe, Steam Oxidation Resistance of Ni-Cr Thermal Spray Coatings on 9Cr-1Mo Steel, Part-2, *ISIJ Int.,* 2003, **43,** p 104-111
10. J.A. Hearley, J.A. Little, and A.J. Sturgeon, The Erosion Behaviour of NiAl Intermetallic Coatings Produced by High Velocity Oxy-Fuel Thermal Spraying, *Wear,* 1999, **233-235,** p 328-333
11. K.J. Stein, B.S. Schorr, and A.R. Marder, Erosion of Thermal Spray MCr–Cr3C2 Cermet Coatings, *Wear,* 1999, **224,** p 153-159

12. "Standard Test Method for Conducting Erosion Tests by Solid Particle Impingement using Gas Jets," D 3565, *Annual Book of ASTM Standards,* ASTM, 2005
13. A.H. Dent, A.J. Horlock, D.G. McCartney, and S.J. Harris, Microstructural Characterisation of a Ni-Cr-B-C Based Alloy Coating Produced by High Velocity Oxy-Fuel Thermal Spraying, *Surf. Coat. Technol.,* 2000, **139,** p 244-250
14. A.J. Sturgeon, Microstructure Characteristics and Corrosion Behaviour of HVOF Sprayed Metallic Coatings, *Thermal Spray 2001: New Surfaces for a New Millennium,* C.C. Berndt, K.A. Khor, and E.F. Lugscheider, Ed., May 28-30, 2001 (Singapore), ASM International, 2001, p 1149-1155
15. N.F. Ak, C. Tekmen, I. Ozdemir, H.S. Soykan, and E. Celik, NiCr Coatings on Stainless Steel by HVOF Technique, *Surf. Coat. Technol.,* 2003, **173-174,** p 1070-1073
16. C. Verdon, A. Karimi, and J.L. Martin, A Study of High Velocity Oxy-Fuel Thermally Sprayed Tungsten Carbide Based Coatings: Part 1. Microstructures, *Mater. Sci. Eng., A,* 1998, **246,** p 11-24
17. H.M. Hawthorne, B. Arsenault, J.P. Immarigeon, J.G. Legoux, and V.R. Parameswaran, Comparison of Slurry and Dry Erosion Behaviour of Some HVOF Thermal Sprayed Coatings, *Wear,* 1999, **225-229,** p 825-834
18. M.A. Uusitalo, P.M.J. Vuoristo, and T.A. Mäntylä, Elevated Temperature Erosion–Corrosion of Thermal Sprayed Coatings in Chlorine Containing Environments, *Wear*, 2002, **252,** p 586-594
19. B. Wang and S.W. Lee, Erosion–Corrosion Behaviour of HVOF NiAl–$Al_2O_3$ Intermetallic-Ceramic Coating, *Wear,* 2000, **239,** p 83-90